

COROTATIONAL GEOMETRICALLY NONLINEAR ANALYSIS OF LAMINATED COMPOSITE SHELLS USING A SHEAR FLEXIBLE TRIANGULAR ELEMENT

Felipe Schaedler de Almeida, schaedleralmeida@gmail.com

Armando Miguel Awruch, awruch@adufrgs.ufrgs

Centro de Mecânica Aplicada e Computacional, Programa de Pós-Graduação em Engenharia Civil,
Universidade Federal do Rio Grande do Sul, Av. Osvaldo Aranha, 99, 3º andar-90035-190, Porto

Abstract. A three-noded triangular flat shell element, used to perform the analysis of laminated composite shell structures, is presented in this work. The finite element is obtained by superposition of a membrane and a plate element. The OPT membrane element, due to Felippa (2003), with corner drilling degrees of freedoms and optimal in-plane bending response, is adopted. The LDT18 plate element, given by Zhang and Kim (2004), is used to complete the shell element. Deflections and rotations on the plate element boundary are defined by the Timoshenko's laminated composite beam function, which provides first-order shear flexibility to the element and naturally avoid shear-locking problems as thin shells are analyzed. Slight transformations are introduced in the original formulation of the plate element, allowing to employ usual corner rotations around local axes. The geometrically nonlinear behavior of the structures is achieved by the element independent corotational formulation (EICR) together with a consistent treatment of finite rotations. Some examples of nonlinear analysis of shell structures are solved using an incremental-iterative method which is able to deal with problems presenting snap-back, snap-through and critical points by automatically sizing the load increment.

Keywords: Laminated composites; Shell structures; Geometrically nonlinear analysis; Finite rotations

1. INTRODUCTION

The growing importance of laminated composites structures has motivated a large number of works related to analysis and design of structures using such materials. The most common kind of composite materials used in the structural field is that formed by a polymeric matrix (usually epoxy), reinforced by high strength/stiffness unidirectional fibers. The orthotropic nature of a lamina made of unidirectional fiber-reinforced composite is reflected in the complex mechanical behavior of the laminates formed by stacking of these laminas with different fiber orientations. Furthermore, it is well known that the effect of transverse shear deformation can be significant, even in thin laminated composite plates or shells. Due to the mechanical behavior and geometrical complexities of laminated composites structures, it is essential to adopt numerical techniques, such as the finite element method.

Flat triangular plate/shell elements are a very practical form of modeling plates and shells. Such type of element is usually computationally efficient and it has a relatively simple formulation. Following this approach, the present work studies the implementation and application of a triangular flat shell element with 18 degrees of freedom (dof), formed by the association of two efficient existing triangular membrane and plate elements, for the nonlinear analysis of laminated composite shells. The membrane formulation is that of the OPT element given by Felippa (2003). Additionally to the in-plane translations degrees of freedom, this element contains a drilling degree of freedom, which is suitable for shell elements. Furthermore, the OPT element showed excellent properties in the case of in-plane bending problems. The plate element used to form the composite shell is given by Zhang and Kim (2004). It consists in an adaptation of a refined 9-dof triangular Mindlin plate element RDKTM (Chen and Cheung, 2000) to the analysis of laminated composite structures. This element is based on the Timoshenko's beam function what provides a unified formulation for thin and thick plates/shells, and naturally avoids shear locking problems.

As long as the linear stiffness matrix of the shell element is formed, the element independent corotational formulation (EICR) is applied to obtain the nonlinear stiffness matrix. The concept of EICR was originally introduced by Rankin and Borgan (1986) and further refined by Rankin and Nour-Omid (1988 and 1991). Extensive discussion about EIRC formulation can be found in Crisfield (1997) and Felippa (2005). The EICR formulation relies heavily in the separation of the rigid body motion and the deformational part of motion and to use projectors to obtain consistent internal force vectors. The consistent treatment of 3D finite rotations is also considered, allowing the analysis of a wider range of problems.

In the next sections the formulation of the membrane and bending parts of the shell element are briefly presented, followed by a discussion on the EIRC nonlinear formulation. Some examples are also present to show the efficiency of the proposed element for the analysis of laminated composite shells.

2. THE TRIANGULAR FLAT SHELL ELEMENT FORMULATION

Figure 1 shows the composition of the shell element by the membrane and plate element and their respective degrees of freedom. All the formulations presented are referred to a local reference system, which has the xy plane coincident with the element plane. The orientation of x and y axes as well as the location of the origin of the reference system are not fixed. Furthermore, the auxiliary geometric constants c_i , b_i , L_i and the area A of the element (they will be used in the following derivations) are calculated as follows:

$$c_i = x_j - x_i, \quad b_i = y_j - y_i, \quad L_i = c_i^2 + b_i^2, \quad A = \frac{1}{2}(c_3b_2 - b_3c_2) \quad (1)$$

The constitutive relation of the laminated composite is considered in this work as given in Eq. (2), where N , M and Q are the integrated stresses thought the section thickness; they are, respectively, the in-plane force vector, the bending moment vector and the shear force vector. The vectors ϵ , κ and γ are the vectors containing mid-plane deformations, curvatures and transverse shearing deformations. Constitutive matrices relating deformation and force components are given by D_m , D_b , D_{mb} and D_s ; they are related to the membrane, bending, coupling membrane-bending and shearing deformations, respectively. The constitutive matrices are obtained by the appropriate integration thought the thickness of the constitutive matrix of each lamina of the laminated composite. All the constitutive matrices given in Eq. (2) are referred to the local reference system, which usually demand some matrix transformations. The laminated composite constitutive matrices and their transformation are well described in many text books like Jones (1999) and Daniel and Ishai (1994), and it will not be discussed in this work.

$$\{N \quad M \quad Q\}^T = \begin{bmatrix} D_m & D_{mb} & 0 \\ D_{mb} & D_b & 0 \\ 0 & 0 & D_s \end{bmatrix} \{\epsilon \quad \kappa \quad \gamma\}^T \quad (2)$$

Using the finite element method, the deformations quantities presented in Eq. (2) can be computed in the domain of each element based on strain-displacement matrices that relate nodal displacements to deformations. This relation is given in Eq. (3), and each strain-displacement is discussed in one of the next specific section of this work. The displacement vectors d_m and d_p contain the membrane and plate displacement, respectively, according to Fig. 1. Only the essential or final equations of the element formulation will be described in the following sections. Reader may found more details about the theoretical aspects and other details in the original references.

$$\{\epsilon \quad \kappa \quad \gamma\}^T = \begin{bmatrix} B_m & 0 & 0 \\ 0 & B_b & B_s \end{bmatrix} \{d_m \quad d_p\}_{element}^T \quad (3)$$

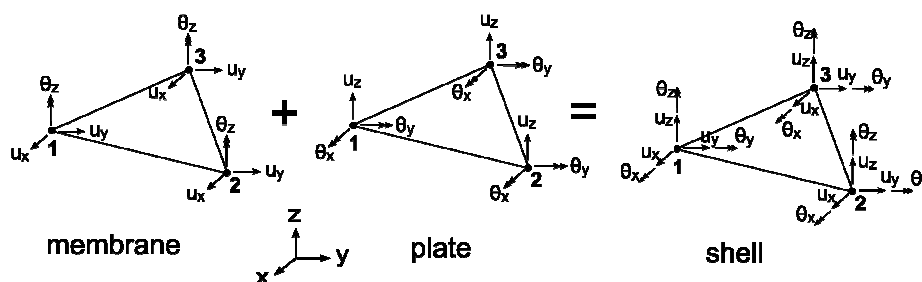


Figure 1. Membrane + plate degrees of freedom = shell degrees of freedom

2.1. The membrane element formulation

As previously mentioned, the formulation adopted for the membrane components of the shell element is that given by Felippa (2003) and called the OPT element. This element has three corners dof per node, two in-plane translations and one drilling rotation. Its development is based on the assumed natural deviatoric strain formulation (ANDES), which lead to the stiffness matrix with free parameters. These parameters have been optimized in order to make the element optimal for in-plane pure bending problems, considering regular meshes of arbitrary aspect ratio. The stiffness matrix is formed by a basic and a hierarchical stiffness matrix, as shown in Eq. (4).

$$K_m = K_m^b + K_m^h \quad (4)$$

The basic stiffness matrix is formed explicitly by the product given in Eq. (5), where \mathbf{B}_m^b is the matrix relating nodal displacements and the mid-plane deformations $\boldsymbol{\varepsilon}$. Equation (6) gives the components of \mathbf{B}_m^b , which consist of geometrical constants and the parameter α_b .

$$\mathbf{K}_m^b = \mathbf{B}_m^{bT} \mathbf{D}_m \mathbf{B}_m^b \quad (5)$$

where

$$\mathbf{B}_m^b = \frac{1}{2A} \begin{bmatrix} b_1 & 0 & \frac{\alpha_b}{6} b_1 (b_3 - b_2) & b_2 & 0 & \frac{\alpha_b}{6} b_2 (b_1 - b_3) & b_3 & 0 & \frac{\alpha_b}{6} b_3 (b_2 - b_1) \\ 0 & c_1 & \frac{\alpha_b}{6} c_1 (c_3 - c_2) & 0 & c_2 & \frac{\alpha_b}{6} c_2 (c_1 - c_3) & 0 & c_3 & \frac{\alpha_b}{6} c_3 (c_2 - c_1) \\ c_1 & b_1 & \frac{\alpha_b}{3} (b_2 c_2 - b_3 c_3) & c_2 & b_2 & \frac{\alpha_b}{3} (b_3 c_3 - b_1 c_1) & c_3 & b_3 & \frac{\alpha_b}{3} (b_1 c_1 - b_2 c_2) \end{bmatrix} \quad (6)$$

The hierarchical stiffness is given in a compact form by:

$$\mathbf{K}_m^h = A \frac{3}{4} \beta_0 \mathbf{T}_{\theta u}^T (\mathbf{Q}_4^T \mathbf{E}_{nat} \mathbf{Q}_4 + \mathbf{Q}_5^T \mathbf{E}_{nat} \mathbf{Q}_5 + \mathbf{Q}_6^T \mathbf{E}_{nat} \mathbf{Q}_6) \mathbf{T}_{\theta u} \quad (7)$$

The matrix $\mathbf{T}_{\theta u}$, given by Eq. (8), relates the nodal displacements to hierarchical rotations used to implement the hierarchical deformational field in the element. Other transformation is performed to obtain the natural stress-strain matrix \mathbf{E}_{nat} , according to Eq. (9), where the natural strain transformation matrix \mathbf{T}_e is also presented.

$$\mathbf{T}_{\theta u} = \frac{1}{4A} \begin{bmatrix} c_1 & -b_1 & 4A & c_2 & -b_2 & 0 & c_3 & -b_3 & 0 \\ c_1 & -b_1 & 0 & c_2 & -b_2 & 4A & c_3 & -b_3 & 0 \\ c_1 & -b_1 & 0 & c_2 & -b_2 & 0 & c_3 & -b_3 & 4A \end{bmatrix} \quad (8)$$

$$\mathbf{E}_{nat} = \mathbf{T}_e^T \mathbf{D}_m \mathbf{T}_e, \quad \mathbf{T}_e = -\frac{1}{4A} \begin{bmatrix} b_1 b_2 L_3 & b_2 b_3 L_1 & b_3 b_1 L_2 \\ c_1 c_2 L_3 & c_2 c_3 L_1 & c_3 c_1 L_2 \\ (c_1 b_2 + b_2 c_1) L_3 & (c_2 b_3 + b_3 c_2) L_1 & (c_3 b_1 + b_1 c_3) L_2 \end{bmatrix} \quad (9)$$

To obtain \mathbf{Q}_4 , \mathbf{Q}_5 and \mathbf{Q}_6 in Eq. (7), the following matrices, as functions of nine dimensionless parameters β_1 to β_9 , are introduced.

$$\mathbf{Q}_1 = \frac{2A}{3} \begin{bmatrix} \frac{\beta_1}{L_3} & \frac{\beta_2}{L_3} & \frac{\beta_3}{L_3} \\ \frac{\beta_4}{L_2} & \frac{\beta_5}{L_2} & \frac{\beta_6}{L_2} \\ \frac{\beta_7}{L_3} & \frac{\beta_8}{L_3} & \frac{\beta_9}{L_3} \end{bmatrix}, \quad \mathbf{Q}_2 = \frac{2A}{3} \begin{bmatrix} \frac{\beta_9}{L_3} & \frac{\beta_7}{L_3} & \frac{\beta_8}{L_3} \\ \frac{\beta_3}{L_2} & \frac{\beta_1}{L_2} & \frac{\beta_2}{L_2} \\ \frac{\beta_6}{L_3} & \frac{\beta_4}{L_3} & \frac{\beta_5}{L_3} \end{bmatrix}, \quad \mathbf{Q}_3 = \frac{2A}{3} \begin{bmatrix} \frac{\beta_5}{L_3} & \frac{\beta_6}{L_3} & \frac{\beta_4}{L_3} \\ \frac{\beta_8}{L_2} & \frac{\beta_9}{L_2} & \frac{\beta_7}{L_2} \\ \frac{\beta_3}{L_3} & \frac{\beta_1}{L_3} & \frac{\beta_2}{L_3} \end{bmatrix} \quad (10)$$

The parameters α_b , β_0 and β_1 to β_9 , presented in Eq. (6), Eq. (7) and Eq. (10), respectively, have been adjusted so that the element is able to produce optimal response for in-plane pure bending deformation. Their values for isotropic materials are given by Eq. (11), where ν is the Poisson's ratio.

$$\alpha_b = \frac{3}{2}, \quad \beta_0 = \max\left[\frac{1}{2}(1-4\nu^2), 0.01\right], \quad \beta_1 = \beta_3 = \beta_5 = 1, \quad \beta_2 = 2, \quad \beta_4 = 0, \quad \beta_6 = \beta_7 = \beta_8 = -1, \quad \beta_9 = -2 \quad (11)$$

According to Felippa (2003), for non-isotropic materials (as is the case of laminated composites), the adoption of the values given in Eq. (11) guarantees that the element will not lock as the aspect ratio increases, although sub-optimal performance can be expected.

Finally, using Eq. (10), it is possible to obtain the matrices \mathbf{Q}_4 , \mathbf{Q}_5 and \mathbf{Q}_6 as follows:

$$\mathbf{Q}_4 = \frac{1}{2}(\mathbf{Q}_1 + \mathbf{Q}_2), \quad \mathbf{Q}_5 = \frac{1}{2}(\mathbf{Q}_2 + \mathbf{Q}_3), \quad \mathbf{Q}_6 = \frac{1}{2}(\mathbf{Q}_3 + \mathbf{Q}_1) \quad (12)$$

Using the above formulation is also possible to determine the strain-displacement matrix, which can be used to obtain strain components with the computed displacement components, or to build a coupling membrane-bending stiffness matrix, as will be discussed latter. In Eq. (13), the coefficient β_0 has been replaced by β_0^e , and the variables ξ_1 , ξ_2 and ξ_3 are the triangular coordinates.

$$\mathbf{B}_m = \mathbf{B}_m^b + \beta_0^e \mathbf{T}_e (\xi_1 \mathbf{Q}_1 + \xi_2 \mathbf{Q}_2 + \xi_3 \mathbf{Q}_3) \mathbf{T}_{\theta_u} \quad (13)$$

In the case where strain components are calculated, the value adopted for β_0^e should be $3/2$ (Felippa, 2003) and for the case where the calculation of the coupling stiffness matrix is desired, the adopted value is $\beta_0^e = \frac{1}{2} \sqrt{\beta_0}$, which allows to obtain the same result of Eq. (4) using Eq. (13) by numerical integration.

2.2. The plate element formulation

The plate element formulation adopted in this work is similar to that given by Zhang and Kim (2004). In the element formulation three auxiliary nodes are used, as shown in Fig. 2. These nodes, with numbers 4, 5 and 6, are placed at the middle of the element sides, and their displacements are obtained by the interpolation of the end nodes displacements. Consideration of both, laminated composite materials and shear flexibility, in the element formulation is achieved using Timoshenko's laminated composite beam function, which is given in Eqs. (14a-b), to obtain, at the mid-side nodes, interpolated values of the transverse displacement w and the plate rotation in the direction of the side coordinate s , denoted by θ_s (see the auxiliary side coordinate s in Fig. 2). The plate rotations in the normal direction to the side, denoted by θ_n , is given by a linear interpolation of its end nodal values (see the auxiliary side coordinate n in Fig. 2). As the rotations θ_s and θ_n are given in terms of side coordinate system, they have to be transformed to the element system. This is performed using the sine sn_a and cosine co_a of the side a with respect to element system, where the side number a is equal to its mid-side node. This transformation is a laborious task which has to be performed for all the intermediate formulation developed based on the side coordinate system, and will not be described in this work. The sine, cosine and length (l_a) of the element sides are given in Eq. (15).

$$w = (\eta_i + \mu \eta_i \eta_j (\eta_i - \eta_j)) w_i + (\eta_i \eta_j + \mu \eta_i \eta_j (\eta_i - \eta_j)) \frac{l}{2} \theta_{s_i} + (\eta_j + \mu \eta_i \eta_j (\eta_j - \eta_i)) w_j - (\eta_i \eta_j + \mu \eta_i \eta_j (\eta_j - \eta_i)) \frac{l}{2} \theta_{s_j} \quad (14a)$$

$$\theta_s = -\frac{6\mu \eta_i \eta_j}{l} w_i + \eta_i (1 - 3\mu \eta_j) \theta_{s_i} + \frac{6\mu \eta_i \eta_j}{l} w_j + \eta_j (1 - 3\mu \eta_i) \theta_{s_j} \quad (14b)$$

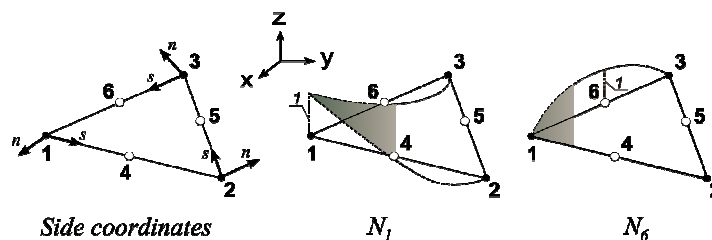


Figure 2. Auxiliary nodes, side coordinates and element interpolation functions

Equation (14a-b) gives the Timoshenko's laminated composite beam function for a beam formed by nodes i and j , lying along an axis s with its origin in i . The variables η_i and η_j are linear functions used to interpolate the nodal displacements of the beam with respect to its end values. Additionally, in Eq. (14a-b), are included the beam length l and the coefficient μ , which consists on a ratio between bending and shearing stiffness. This coefficient determines the effect of shear deformation in the beam displacement. For the plate element formulation a coefficient μ_a must be determined for each side, considering its local orientation and the stress-strain matrices \mathbf{D}_b and \mathbf{D}_s , which are referred to de elements system. Equation (16) gives μ_a for each side, being λ_a an auxiliary variable.

$$sn_4 = \frac{-c_3}{l_4}, \quad sn_5 = \frac{-c_2}{l_5}, \quad sn_6 = \frac{-c_2}{l_6}, \quad co_4 = \frac{-b_3}{l_4}, \quad co_5 = \frac{-b_2}{l_5}, \quad co_6 = \frac{-b_2}{l_6} \quad (15)$$

$$l_4 = \sqrt{L_3}, \quad l_5 = \sqrt{L_1}, \quad l_6 = \sqrt{L_2}$$

$$\mu_a = \frac{1}{1-12\lambda_a}, \quad \lambda_a = \frac{D_{b11}co_a^4 + 2(D_{b12} + 2D_{b33})co_a^2sn_a^2 + D_{b22}sn_a^4}{l_a^2(D_{11}co_a^2 + 2D_{12}sn_a co_a + D_{s22}sn_a^2)} \quad (16)$$

As the displacements in the mid-side nodes are known interpolating corner nodal displacements using the Timoshenko's laminate beam function, a set of interpolation functions can be used to form the rotational field in the element domain, as given in Eq. (17). The shape functions N_i and N_a for corner and mid-side nodes, respectively, are represented in Fig. 2 for nodes 1 and 6. In every equation related to a mid-side node $a=4, 5, 6$ the corresponding values of $i-j$ are 1-2, 2-3 and 3-1, respectively.

$$\begin{Bmatrix} \theta_x \\ \theta_y \end{Bmatrix} = \sum_{i=1}^3 N_i \begin{Bmatrix} \theta_x \\ \theta_y \end{Bmatrix}_{node_i} + \sum_{a=4}^6 N_a \begin{Bmatrix} \theta_x \\ \theta_y \end{Bmatrix}_{node_a}, \quad N_i = (2\xi_i - 1)\xi_i, \quad N_a = 4\xi_i\xi_j \quad (17)$$

Once the rotation field is established in the element, the bending strain-displacement matrix can be obtained by differentiation of the shape functions N_i and N_a . Only the final results are presents here, introducing for this purpose the intermediate matrices $\bar{\mathbf{T}}_a$, $\bar{\mathbf{L}}_a$, $\bar{\mathbf{L}}\mathbf{T}_a^1$ and $\bar{\mathbf{L}}\mathbf{T}_a^2$, calculated for each mid-side node $a=4,5,6$, and $\hat{\mathbf{L}}_i$, calculated for each corner node $i=1,2,3$. The matrix $\bar{\mathbf{T}}_a$, which contains only properties depending of geometrical and material characteristics is given by Eq. (18). It is worthy to point out that this matrix can be calculated only once when a numerical integration process is used to form the stiffness matrix.

$$\bar{\mathbf{T}}_a = \begin{bmatrix} -\frac{3}{2}\mu_a sn_a / l_a & -\frac{3}{4}\mu_a sn_a co_a & -\frac{3}{4}\mu_a sn_a^2 + \frac{1}{2} \\ \frac{3}{2}\mu_a co_a / l_a & \frac{3}{4}\mu_a co_a^2 - \frac{1}{2} & \frac{3}{4}\mu_a sn_a co_a \end{bmatrix} \quad (18)$$

Matrix $\bar{\mathbf{L}}_a$ is given by Eq. (19). In this case the triangular coordinates are used for the matrix calculation and then a new calculation must be performed for each point used in the numerical integration.

$$\bar{\mathbf{L}}_a = \begin{bmatrix} \bar{b}_a & 0 & \bar{c}_a \\ 0 & \bar{c}_a & \bar{b}_a \end{bmatrix}^T, \quad \bar{b}_a = \frac{2}{A}(b_i\xi_j - b_j\xi_i), \quad \bar{c}_a = \frac{2}{A}(c_i\xi_j - c_j\xi_i) \quad (19)$$

After matrices given in Eq. (18) and Eq. (19) are calculated their results are combined to form $\bar{\mathbf{L}}\mathbf{T}_a^1$ and $\bar{\mathbf{L}}\mathbf{T}_a^2$. The resulting matrix $\bar{\mathbf{L}}\mathbf{T}_a^1$ is obtained by the product in Eq. (20), while $\bar{\mathbf{L}}\mathbf{T}_a^2$ is obtained by changing the sign of the first column of $\bar{\mathbf{L}}\mathbf{T}_a^1$.

$$\bar{\mathbf{L}}\mathbf{T}_a^1 = \bar{\mathbf{L}}_a \bar{\mathbf{T}}_a \quad (20)$$

The reminder matrix, relative to the corner nodes, is formed as shown in Eq. (21).

$$\hat{\mathbf{L}}_i = \begin{bmatrix} 0 & 0 & \hat{b}_i \\ 0 & -\hat{c}_i & 0 \\ 0 & -\hat{b}_i & \hat{c}_i \end{bmatrix}, \quad \hat{b}_i = \frac{b_i}{2A}(4\xi_i - 1), \quad \hat{c}_i = \frac{c_i}{2A}(4\xi_i - 1) \quad (21)$$

Finally, when all intermediate matrices were calculated, the bending strain-displacement matrix \mathbf{B}_b , as given in Eq. (22), can be obtained easily.

$$\mathbf{B}_b = [\mathbf{B}_{b1} \quad \mathbf{B}_{b2} \quad \mathbf{B}_{b3}], \quad \mathbf{B}_{b1} = \hat{\mathbf{L}}_1 + \bar{\mathbf{L}}\mathbf{T}_4^1 + \bar{\mathbf{L}}\mathbf{T}_6^2, \quad \mathbf{B}_{b2} = \hat{\mathbf{L}}_2 + \bar{\mathbf{L}}\mathbf{T}_5^1 + \bar{\mathbf{L}}\mathbf{T}_4^2, \quad \mathbf{B}_{b3} = \hat{\mathbf{L}}_3 + \bar{\mathbf{L}}\mathbf{T}_6^1 + \bar{\mathbf{L}}\mathbf{T}_4^2 \quad (22)$$

The shear strain-displacement relation is developed in the element formulation in a way very similar to that used to obtain the bending contribution. As in the previous case, when bending was analyzed, only the final results are shown here. Two auxiliary matrices are introduced in Eq. (23a-b) and Eq. (24a-b). The first one is a matrix which depends of geometric and material characteristics, while the second one takes into account the triangular coordinates.

$$\bar{\mathbf{H}} = \begin{bmatrix} h_4 & ch_4 & sh_4 & -h_4 & ch_4 & sh_4 & 0 & 0 & 0 \\ 0 & 0 & 0 & h_5 & ch_5 & sh_5 & -h_5 & ch_5 & sh_5 \\ -h_6 & ch_6 & sh_6 & 0 & 0 & 0 & h_6 & ch_6 & sh_6 \end{bmatrix} \quad (23a)$$

where, for each mid-side node $a=4,5,6$,

$$h_a = \frac{\mu_a - 1}{l_a}, \quad sh_a = \frac{1}{2} sn_a (\mu_a - 1), \quad ch_a = \frac{1}{2} co_a (\mu_a - 1) \quad (23b)$$

$$\bar{\mathbf{N}} = \begin{bmatrix} co_6 a_1^* - co_5 a_2^* & co_4 a_2^* - co_6 a_3^* & co_5 a_3^* - co_4 a_1^* \\ sn_6 a_1^* - sn_5 a_2^* & sn_4 a_2^* - sn_6 a_3^* & sn_5 a_3^* - sn_4 a_1^* \end{bmatrix}, \quad (24a)$$

with

$$a_1^* = \frac{\xi_1}{co_4 sn_6 - co_6 sn_4}, \quad a_2^* = \frac{\xi_2}{co_5 sn_4 - co_4 sn_5}, \quad a_3^* = \frac{\xi_3}{co_6 sn_5 - co_5 sn_6} \quad (24b)$$

The shear strain-displacement matrix can then be obtained by the product of the two auxiliary matrices (Eqs. 23a and 24a), as given in Eq. (25).

$$\mathbf{B}_s = \bar{\mathbf{N}} \bar{\mathbf{H}} \quad (25)$$

The plate stiffness matrix is formed by the bending and shearing contributions. Eq. (26) shows the summation of this two parts which may be obtained by numerical integration in the element domain.

$$\mathbf{K}_p = \mathbf{K}_b + \mathbf{K}_s = \int_A \mathbf{B}_b^T \mathbf{D}_b \mathbf{B}_b dA + \int_A \mathbf{B}_s^T \mathbf{D}_s \mathbf{B}_s dA \quad (26)$$

2.3. The shell element stiffness matrix

Once the strain-displacement matrices are defined, it is possible to obtain the complete shell stiffness matrix as presented in Eq. (27). The calculation of the components \mathbf{K}_m and \mathbf{K}_b have been demonstrated in the previous sections. However, due to the membrane-bending coupling stress-strain matrix \mathbf{D}_{mb} , which is present in non symmetric laminates, two additional stiffness components, \mathbf{K}_{mb} and \mathbf{K}_{bm} , appears.

$$\mathbf{K} = \int_A \begin{bmatrix} \mathbf{B}_m^T & 0 \\ 0 & \mathbf{B}_b^T \\ 0 & \mathbf{B}_s^T \end{bmatrix} \begin{bmatrix} \mathbf{D}_m & \mathbf{D}_{mb} & 0 \\ \mathbf{D}_{mb} & \mathbf{D}_b & 0 \\ 0 & 0 & \mathbf{D}_s \end{bmatrix} \begin{bmatrix} \mathbf{B}_m & 0 & 0 \\ 0 & \mathbf{B}_b & \mathbf{B}_s \end{bmatrix} = \begin{bmatrix} \int_A \mathbf{B}_m^T \mathbf{D}_m \mathbf{B}_m & \int_A \mathbf{B}_m^T \mathbf{D}_{mb} \mathbf{B}_b \\ \int_A \mathbf{B}_b^T \mathbf{D}_{mb} \mathbf{B}_m & \int_A \mathbf{B}_b^T \mathbf{D}_b \mathbf{B}_b + \int_A \mathbf{B}_s^T \mathbf{D}_s \mathbf{B}_s \end{bmatrix} = \begin{bmatrix} \mathbf{K}_m & \mathbf{K}_{mb} \\ \mathbf{K}_{bm} & \mathbf{K}_p \end{bmatrix} \quad (27)$$

These coupling stiffness matrices can be obtained by the integration given in Eq. (27). The symmetric characteristic of the stiffness matrix can be used, so that only one of the two matrices, \mathbf{K}_{mb} or \mathbf{K}_{bm} , is calculated, since one matrix is equal to the transpose of the other one. The formulation described until now has considered a separation between membrane and plate displacements, \mathbf{d}_m and \mathbf{d}_p , respectively, as shown in Fig. 1. However, for a global implementation, it is necessary to work with a displacement vector and a corresponding internal force vector, as in Eq. (28). This change of the displacement components organization demands a reallocation of the components in the shell stiffness matrix, which result in a mixing of the membrane, plate and coupling stiffness matrices elements. These elements were originally separated.

$$d = \{d_1 \quad d_2 \quad d_3\}^T, \quad d_i = \{u_1 \quad u_2 \quad u_3 \quad \theta_1 \quad \theta_2 \quad \theta_3\}^T \\ f = \{f_1 \quad f_2 \quad f_3\}^T, \quad f_i = \{n_1 \quad n_2 \quad n_3 \quad m_1 \quad m_2 \quad m_3\}^T \quad (28)$$

3. THE ELEMENT INDEPENDENT COROTATIONAL FORMULATION

The element independent corotational formulation (EICR) is a systematic procedure used to extend the capabilities of existing linear finite elements to problems concerning finite rotations (Nour-Omid and Rankin, 1991). The main idea of the corotational formulation is to define a local coordinate system, which rotates and translates attached to the finite element. When using the EICR formulation, separation of the element rigid body motion from the deformational part of the total element displacement occurs before any element computation is performed. As this pre-processing of displacements step is made outside standard finite element routines it is almost independent of the element type (Felippa, 2005). After deformational displacements are isolated it is possible to obtain the local internal force vector using the element stiffness matrix, which is calculated by the standard linear formulation. Both, internal force vector and stiffness matrix, are then transformed generating global consistent values.

In a finite rotation analysis the nodal rotations are represented by an orthogonal matrix \mathbf{R}_i , which defines the displacement for a node i together with the translational displacement vector (\mathbf{u}_i). Considering the well known local-to-global displacement transformation matrix \mathbf{T}_n , given for a specific element at a configuration n , the nodal deformational displacements for each element is obtained by the expression given by Eq. (29a) and Eq. (29b).

$$\mathbf{u}_i^d = \mathbf{T}^T (\mathbf{y}_i - \mathbf{y}_c) - \mathbf{T}_0^T (\mathbf{x}_i - \mathbf{x}_c), \quad \mathbf{y}_i = \mathbf{x}_i + \mathbf{u}_i^n \quad (29a)$$

$$\boldsymbol{\theta}_i^d = \ln(\mathbf{T}_n \mathbf{R}_i \mathbf{T}_0^T) \quad (29b)$$

In Eq. (29a) y and x are the nodal position for configurations n and 0 , respectively. The subscript c is referred to the point located at the element center, which is also the origin of the local system. The element center is given by the mean value of the element nodes position. In Eq. (29b) the orthogonal matrix obtained by the matrix product in the logarithmic expression is transformed to an equivalent rotation vector by a procedure equivalent to the logarithm calculation. This procedure lies on complicated mathematical foundations and is well described in Felippa (2005) or Crisfield (1997). The transformation of the local element internal force vector to a consistent global internal force vector is given in Eq. (30). This transformation results from the following subsequent operations: change of rotational variables, originating the matrix \mathbf{H} ; elimination of rigid body motion, originating the projector \mathbf{P} ; finally, local to global transformation, given by \mathbf{T} . The superscript g and l define variables referred to the global and local systems, respectively, and the vector \mathbf{d}^d is the local deformational displacement vector formed using the results of Eq. (29a-b).

$$\mathbf{f}^g = \mathbf{T}^T \mathbf{P}^T \mathbf{H}^T \mathbf{f}^l, \quad \mathbf{f}^l = \mathbf{K}^l \mathbf{d}^d \quad (30)$$

The nonlinear stiffness matrix at element level is given in the global reference system by the variation of the internal force vector, given in Eq. (30), with respect to global displacements. Equation (31) gives this relation in a compact form, where the matrix product in the right hand side of this equation gives the material component of the nonlinear stiffness and \mathbf{K}_σ is the geometric component originated by the derivations of \mathbf{H} , \mathbf{P} and \mathbf{T} . Detailed discussion on the formation of the above mentioned matrices and other aspects of the EIRC formulation involve complex or at least extensive derivations and details will be not presented in this work. Comprehensive treatment of nonlinear static and dynamic problems can be found in many research works, being worthy to cite the works of Felippa (2005) and Crisfield (1997).

$$\mathbf{K}^g = \frac{\partial^2 \mathbf{f}^g}{\partial \mathbf{d}^g} = \mathbf{T}^T \mathbf{P}^T \mathbf{H}^T \mathbf{K}^l \mathbf{H} \mathbf{P} \mathbf{T} + \mathbf{K}_\sigma \quad (31)$$

4. EXAMPLES

In this section three examples applying the theory, which has been previously discussed, are presented. Dimensionless unities are used for all the examples. The first and the second examples laminated composite shells with geometrically nonlinear behavior are analyzed. An incremental iterative method with automatic step sizing and path-follow capability, due to Yang and Shieh (1990), is adopted for the solution of the nonlinear problem. These examples were taken from a benchmark paper (Sze et al., 2004), where the results of the analyses obtained using different meshes of quadrilateral elements are presented, allowing an accurate reproduction of the load-deflection curves. In both examples the 0° oriented fibers are aligned to the global axis x . The third example shows a comparison between the proposed element and a similar element, with a different membrane formulation, in the analysis of a problem where in-plane bending occurs.

4.1. Pinched semi-cylindrical laminated shell

The semi-cylindrical shell showed in Fig. 3 is subject to a downward force $P=2000$ in the top of its free edge, while its other edge is fully clamped. Two laminates with stacking sequences $(90^\circ/0^\circ/90^\circ)$ and $(0^\circ/90^\circ/0^\circ)$ are considered, with

all plies having the thickness $t=1$. The mechanical properties for the longitudinal (L) and transverse (T) to the fibers directions are given by: $E_L=2068.5$, $E_T=517.125$, $G_{LT}=795.6$ and $\nu_{LT}=\nu_{TT}=0.3$, where E is the Young's modulus, G is the shear modulus and ν is the Poisson's ratio. The geometric characteristic dimensions are the length $L=304.8$ and the radius $R=101.6$. Thanks to the geometrical and material symmetry only half of the shell is analyzed. This example is useful to demonstrate the ability of the formulation adopted by this work in solving nonlinear problems with large rotations and displacements, since the final displacement of point A is more than 1.5 times greater than the radius R .

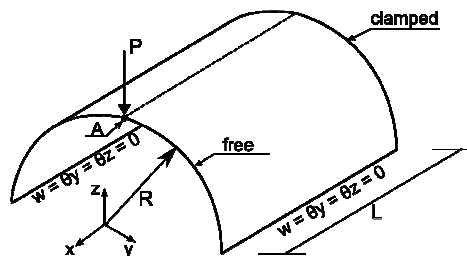


Figure 3. Semi-cylindrical shell

Figure 4a shows the comparison between the results obtained in the present work and those given by Sze et al. (2004). The load-deflection curves obtained at the point A (see Fig. 3) agree very well with the benchmark data. Both results were obtained by a 40x40 regular mesh with the same number of nodes. A second investigation compares the result of the present implementation by modeling the structure with a 40x40 fine mesh and a 16x24 coarse mesh. Figure 4b shows that even with a coarse mesh (with about 1/4 of the elements and nodes of the fine mesh) very good results can be obtained.

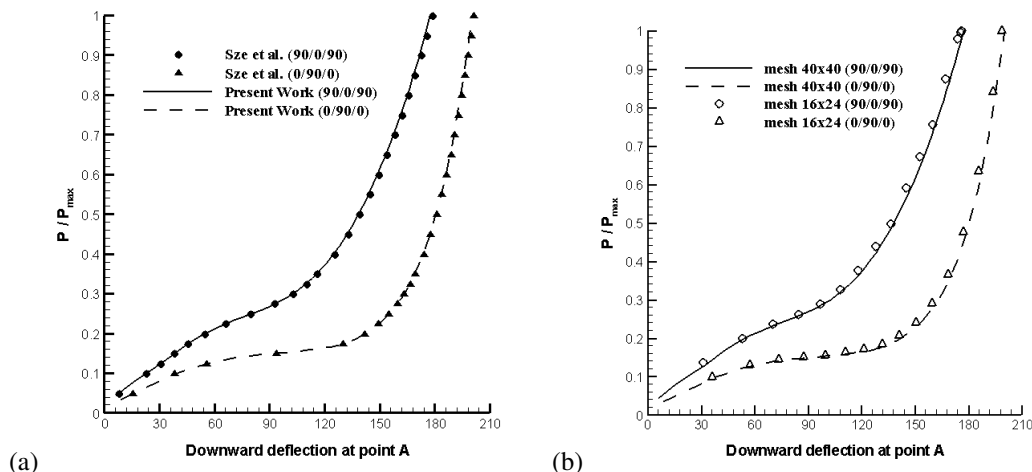


Figure 4. (a) Results of the present work and comparison with a benchmark. (b) Results using a coarse and a fine mesh.

4.2. Hinged cylindrical laminated roof

This example is depicted in Fig. 5, where the semi-cylindrical roof is presented with its boundary conditions and geometrical parameters. Two laminates with stacking sequences $(90^\circ/0^\circ/90^\circ)$ and $(0^\circ/90^\circ/0^\circ)$ and total thickness $h=6.35$ are considered. The mechanical properties are given by: $E_L=3300$, $E_T=1100$, $G_{LT}=660$ and $\nu_{LT}=\nu_{TT}=0.25$. A downward load is applied at the center of the shell, in point A.

This example is very popular in the literature due to the high nonlinear behavior of the structure with the presence of snap-through and snap-back phenomena. It is a very good test to demonstrate the ability of the implemented algorithm in solving strongly nonlinear problems. Due to the symmetry, only one quarter of the structures have been modeled by a 24x24 mesh. This mesh has the same number of nodes of the mesh used in the reference work. Figure 6a shows the results obtained by the present work and those presented by the reference for the laminate $(0^\circ/90^\circ/0^\circ)$, while Fig. 6b shows the results for the laminate $(90^\circ/0^\circ/90^\circ)$. As in the first example, results agree very well with the benchmark data, with a very small divergence at the end of the loading.

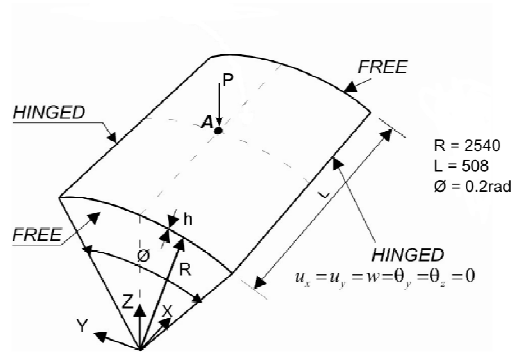


Figure 5. Hinged cylindrical laminated roof

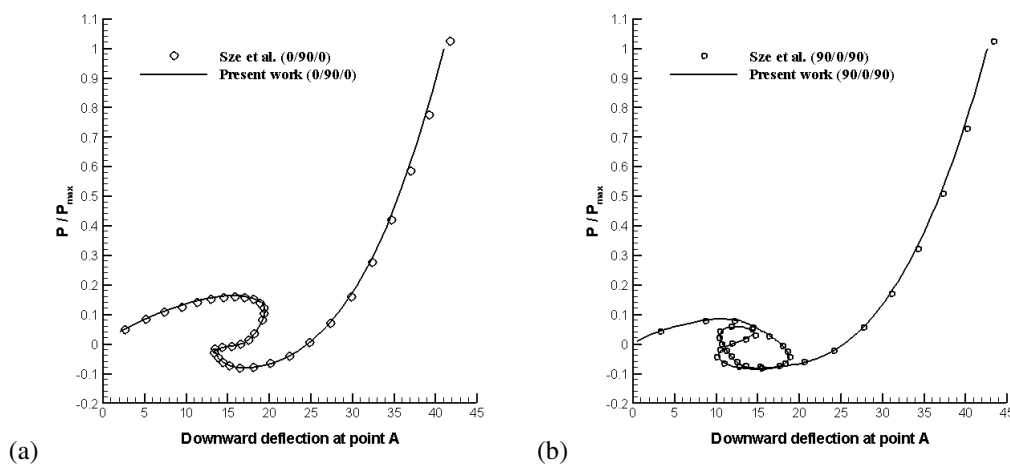


Figure 6. Load-deflection curve for the laminates with stacking sequences: (a) $(0^\circ/90^\circ/0^\circ)$ and (b) $(90^\circ/0^\circ/90^\circ)$

4.3. Clamped plate with a stringer

Figure 7 shows the structure to be analyzed in this example. It consists on a long plate with length $L=10$ and width $b=1$, stiffened by a stringer of height $h=0.1$. The plate is clamped in one of its shorter sides and subject to a vertical load $P=1$ at the opposite side. Different to the last examples, the material in this case is isotropic with mechanical properties: $E=120 \cdot 10^6$, $G=60 \cdot 10^6$ and $\nu=0.0$. Both plate and stringer have thickness $t=0.01$.

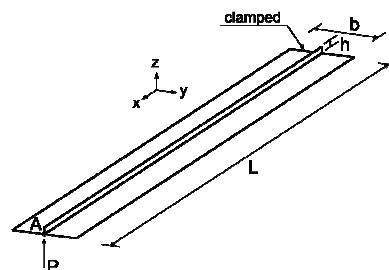


Figure 7. Clamped plate with a stringer

The objective of this example is to verify the advantage of using the OPT element as membrane component in triangular flat shell elements when in-plane bending deformation is observed. This advantage was widely demonstrated by Felippa (2003) for linear analysis, and has been verified by Battini and Pascote (2006) for corotational nonlinear analysis of shells. The present work compare the OPT element to the widely used ALL element (Allman, 1988), which has the same number of nodes and *dof* of the OPT element. Table 1 shows the vertical deflection of point A at the end of the loading process in the nonlinear analysis. To avoid any influence of the solution method in the final result, the traditional Newton-Raphson incremental-iterative procedure is used with 20 equal load steps. The comparison is made for different structured meshes designated by the number of division of the structure in the x, y and z directions (or

along L , b and h), denoted by $n_x/n_y/n_z$. All meshes are defined to give an unitary aspect ratio for the plate elements, $\lambda_p=1$, while the aspect ratio of the stringer elements λ_s may vary for the different meshes. The number of elements used to model the stringer and the aspect ratio of these elements are also showed in Table 1. A very fine mesh 400/40/4, with 35200 elements and 18045 nodes, was used to obtain a reference displacement for each case. However, even for this mesh, different results were obtained using the OPT and ALL elements. Unless for meshes with $\lambda_s=5$, all the solutions using the OPT element gave results differing less than 0.6% with the reference results, while the displacement obtained with the coarsest mesh differs less than 8% from the displacement given in the reference. On the other hand, in the different analyses performed using the ALL element, only fine meshes, with at least 400 stringer elements, were able to produce results differing 5.8% to 7% from the reference values. As observed by Felippa (2003), for linear analysis, the ALL element exhibit catastrophic aspect ratio locking in the problem studied here, with the worst value differing 62% from the reference value. Furthermore, coarse meshes lead to unacceptable results even for good aspect ratios.

Table 1. Comparison of displacement at point A using ALL and OPT shells elements for different meshes.

$n_x/n_y/n_z$	stringer elements	λ_s	ALL	OPT
20/2/1	40	5	0.334677	0.807845
40/4/1	80	2.5	0.590612	0.870239
40/4/2	160	5	0.607088	0.85095
100/10/1	200	1	0.750071	0.87679
100/10/2	400	2	0.806374	0.875223
100/10/3	600	3	0.814589	0.874341
100/10/4	800	4	0.81641	0.873186
100/10/5	1000	5	0.816447	0.871755
400/40/4	3200	1	0.866944	0.876082

5. CONCLUSIONS

The formulation of a triangular flat shell element composed by efficient membrane and plate elements was concisely presented. Both, membrane and plate elements formulations have been derived using the same geometrical constants and following steps that make its implementation in a computational code straightforward. Results of the numerical examples presented here have shown excellent agreement with respect to the references. This was observed for a problem with large rotations and displacements and for a highly nonlinear problem. In the third example the advantage of using the OPT element as the membrane component of the shell element was demonstrated. Good results were obtained even for coarse meshes. When compared to ALL, a widely used membrane element, the OPT element has always shown better results.

6. REFERENCES

- Allman, D.J., 1988, "Evaluation of the constant strain triangle with drilling rotations", *Int. J. Numer. Methods Engrg.* Vol. 26, pp. 2645–2655.
- Chen, W.J., Cheung, Y.K., 2001 "Refined 9-dof triangular Mindlin plate elements", *Int. J. Numer. Methods Engrg.* Vol. 51, pp. 1259–128
- Daniel, I.M., Ishai, O., 1994, "Engineering Mechanics of Composite Materials", Oxford University Press, 1994.
- Felippa, C.A., 2003 "A study of optimal membrane triangles with drilling freedoms", *Comp. Meth. App. Mech. Eng.*, Vol. 192, pp. 2125-2168.
- Felippa, C.A., Haugen, B., 2005 "A unified formulation of small-strain corotational finite elements: I. Theory", *Comp. Meth. App. Mech. Eng.*, Vol. 194, pp. 2285-2335.
- Jones, R.M., 1999, *Mechanics of Composite Materials*, 2^oEd. Hemisphere, New York.
- Nour-Omid, B., Rankin, C. C., 1991, "Finite rotation analysis and consistent linearization using projectors", *Computer Methods in Applied Mechanics and Engineering*, Vol. 93, No. 3, pp. 353-384.
- Rankin, C. C., and Nour-Omid, B., 1988, "The use of projectors to improve finite element performance", *Computers & Structures*, Vol. 30, pp. 257–267.
- Rankin, C. C., and Brogan, F.A., 1986, "An element-independent corotational procedure for the treatment of large rotations", *ASME J. Pressure Vessel Technology*, 108, 165–174.
- Sze, K.Y. ; Liu, H. ; Lo, S.H., 2004, "Popular benchmark problems for geometric nonlinear analysis of shells." *Finite Elements in Analysis and Design*. Vol. 40, pp. 1551–1569.
- Yang, Y., Shieh, M., 1990, "Solution Method for Nonlinear Problems with Multiple Critical Points." *AIAA JOURNAL*, Vol. 28, No. 12, pp. 2110-2116.
- Zhang, Y.X., Kim, K.S., 2005, "A simple displacement-based 3-node triangular element for linear and geometrically nonlinear analysis of laminated composite plates", *Comp. Meth. App. Mech. Eng.*, Vol. 194, pp. 4607-4632.